Int. J. Heat Mass Transfer. Vol. 19, pp. 285–295. Pergamon Press 1976. Printed in Great Britain

DISPERSION MEASUREMENTS IN A TURBULENT BOUNDARY LAYER

D. J. SHLIEN† and S. CORRSIN
Department of Mechanics and Materials Science, The Johns Hopkins University, Baltimore, MD 21218, U.S.A.

(*Received* 18 *August* 1974 *and in revised form* 1 *April* 1975)

Abstract—Dispersion in a turbulent boundary layer was measured in a wind tunnel, downstream of a long heated wire located (successively) at the wall, at 1.66 displacement thickness from the wall, at the position beyond which the intermittency drops below 1.0, and in the intermittent region. Mean temperature profiles approached nearly the same asymptotic shape in all cases. A turbulent Prandtl number, defined by

$$\left[\frac{U_\infty}{v_t}\frac{\partial}{\partial x}\tfrac{1}{2}\overline{(Y-\bar{Y})^2}\right]^{-1}$$

was not far from the "Reynold analogy" value of 1 (0·6 to 0·8). Furthermore this turbulent Prandtl number was approximately independent of downstream position and showed little variation with source distance from the wall. Mean wall concentrations (temperatures) as a function of downstream distance were fitted with simple power laws. The constant b in Batchelor's [1, 2] theory for the mean particle displacement perpendicular to the wall was calculated from the wall source data, although a basic hypothesis of the theory ($\bar{V} \approx$ constant), was contradicted by the data. The b value agreed closely with the estimates of Ellison [3] and Pasquill [4]. Restrictions of the theory were not satisfied for the other source positions. Comparisons with Poreh and Cermak's [5] measurements (at about the same Reynolds number) showed some areas of agreement.

NOMENCLATURE

A, a constant of integration, see equation (3);
b, Batchelor's constant, see equation (1);
c, an assumed constant, see equation (2);
d_T, tagging wire diameter;
Q, $\equiv \int_0^\infty \frac{\bar{U}(y)}{U_\infty}\theta(y)\,dy$, mean heat flux;
u^*, square root of the wall shear stress divided by the fluid density;
$\bar{U}$, mean streamwise velocity;
U_∞, free stream velocity;
v, velocity fluctuation component perpendicular to the wall;
$\bar{V}$, $\frac{d\bar{Y}}{dt}$;
$x, \Delta x$, streamwise distance from the secondary contraction exit and from the tagging wire, respectively;
$\bar{X}(t)$, mean downstream particle displacement;
y, distance from the wall;
y_T, tagging wire distance from the wall;
Y, tagged particle distance from the wall;
$\Delta\bar{Y}$, $\equiv \bar{Y}-y_T$.

Greek symbols

γ, intermittency, i.e. fraction of the time flow is turbulent;
$\delta, \delta_d, \delta_d^T$, 99 per cent boundary-layer thickness, displacement thickness and displacement thickness at the tagging wire position, respectively;
κ, von Kármán constant, 0·41;
v_t, typical boundary layer "eddy viscosity";
ϑ, temperature fluctuation;
$\bar{\theta}(x, y), \bar{\theta}_p(x), \bar{\theta}_w(x)$, mean temperature, peak value, and wall value respectively.

Superscript

$\bar{}$, averaged quantity.

1. INTRODUCTION

THE DISPERSION of a passive contaminant by turbulence not only is intrinsically interesting but is fundamental to practical heat- and mass-transfer problems. In flows other than the simplest ones very little progress has been made towards sound theoretical predictions. The greatest success has been with phenomenological models like those employing turbulent (or eddy) diffusivities but the principle behind this concept is wrong (see for example, Batchelor [6], Corrsin [7, 8]). An example of turbulent diffusivity models is given by Morkovin [9] who showed that, when viewed as properties of quasi-similar fields, eddy diffusivities can account for some observed characteristics of a thermal boundary layer developing in a turbulent boundary layer.

Few measurements of dispersion of a passive contaminant in a boundary layer have been made under the controlled conditions of the laboratory. One of the earliest of these was by Skramstad and Schubauer [10]

†Present address: Tel-Aviv University, School of Engineering, Ramat Aviv, Israel.

as reported in more detail by Dryden [11]. Mean temperatures were measured behind a heated wire in a boundary layer, but only for relatively short distances (maximum downstream distance was approximately $\frac{1}{2}\delta$). Wieghardt [12] measured dispersion from a "point" source (3×32 mm) as well as a line source of heat on the boundary layer wall for distances up to approximately ten boundary-layer thicknesses ($\delta =$ 4·9–8·6 cm). Other measurements of dispersion from *point* sources include those by Kesic [13], Chandra [14] and Chaudhry and Meroney [15].

Johnson [16, 17] measured mean temperature profiles and statistics of temperature fluctuations in a turbulent boundary layer for a small stepwise discontinuity in the wall temperature. The heated wall was not long enough for the thermal boundary layer to grow out to the free stream. He found that the instantaneous surface of demarkation between the heated and unheated fluid was sharp and distinct. The local turbulent Prandtl number was calculated at one downstream section and was found to vary between 0·8 and 1·2. Similarly, Nicholl [18] investigated the dynamical effects of a strong discontinuity in the floor or roof temperature of a wind tunnel, and Trinite and Valentin [19] measured temperature and concentration profiles downstream of a stepwise discontinuity in wall temperature and concentration. Further discussion and other references on dispersion in a turbulent boundary layer is found in the book by Monin and Yaglom [20] (Sections 9.4 and 10).

In this paper, measurements of mean temperature profiles downstream of a long heated wire normal to the flow and parallel to the wall, are reported. The RMS values, skewnesses, micro- and integral scales, and probability distributions of temperature fluctuations were measured at two sections in the boundary layer, along with probability distributions of pulse and gap widths of the (intermittent) temperature signal. These have been reported by Shlien [21] and will be published in the future.

2. POREH AND CERMAK'S EXPERIMENTS AND BATCHELOR'S THEORY

Poreh and Cermak [5] measured the dispersion of ammonia gas from a steady line source normal to the flow, on the wall of a turbulent boundary layer. Data were reproducible within a deviation of about 10 per cent. Four stages of dispersion development were discussed:

(i) The initial stage has large velocity gradients (near the wall) and large concentration gradients.

(ii) In the intermediate stage "the diffusing plume ... is submerged in the boundary layer", that is, dispersion is unaffected by (or the contaminant has not dispersed to) the turbulent–irrotational interface.

(iii) A stage of transition from the intermediate stage to the final one. The turbulent–irrotational interface behaves like a "lid" allowing dispersion through it only by the relatively slow process of molecular diffusion, which is, of course, greatly enhanced by the turbulent "stretching" of constant concentration surfaces, analogous to the Corrsin–Kistler [22] mechanism for viscous propagation of vorticity via the "laminar superlayer".

(iv) In the final (asymptotic) stage, dispersion "is limited by the growth of the developing boundary layer" (Poreh and Hsu [23]). All the contaminant is contained by the wall and the turbulent–irrotational interface.

Poreh and Cermak's measurements extended from within the intermediate stage to within the final one, that is, from $\Delta x \approx 35\delta_d^T$ to $1340\delta_d^T$, where $\delta_d^T \equiv \delta_d$ at $\Delta x = 0$; $\delta \approx 6{\cdot}6\delta_d$. Two source positions (7·8 and 2·3 m downstream of the boundary-layer trip called series I and II respectively) and three free stream velocities were used resulting in Reynolds number (based on δ_d^T) ranges of 5200 6800 for "series I" and 2500–3300 for "series II". For the intermediate stage they found that the mean concentration, normalized with its maximum C/C_M, equals $f(\xi)$ where $\xi = y/y_{0\cdot5}$ such that $f(1) = 0{\cdot}5$ and that $C_M \propto \Delta x^{-0\cdot9}$. For the final stage, $C/C_M = F(\eta)$ and $C_M \propto \Delta x^{-1\cdot0}$ where $\eta = y/\delta$.

Collapsing the intermediate stage data with C_M and $y_{0\cdot5}$ normalizations is an insensitive determination of quasi-similarity (Morkovin's [9] term) since two points on a monotonic decreasing curve having zero slope at $\xi = 0$ are forced to coincide—the $\xi = 0$ point and the $C = 1/2C_M$ point. Another problem with using $y_{0\cdot5}$ as a characteristic length of the mean concentration profiles is the sensitivity of its value to data scatter. This resulted in 22 per cent variations in the ratio of $y_{0\cdot5}$ to the centroid of the concentration profile for the intermediate stage. Other characterizations of the mean concentration (or temperature) profiles will be presented here.

In 1959, Batchelor [1] first presented the idea of applying similarity to dispersion in a turbulent boundary layer. This idea was taken up, tested and extended by Ellison [3], Gifford [24] and Cermak [25]. Then in 1964, Batchelor [2] again presented the basic idea, with some minor improvements. He assumed similarity of a form such that the statistical properties of the Lagrangian velocity depend only on u^* and time (valid for the constant stress region) resulting in

$$\overline{V} \equiv \frac{\mathrm{d}\overline{Y}}{\mathrm{d}t} = bu^* \tag{1}$$

where b is an "absolute" constant. He also assumed that a constant c (of order unity) exists such that the mean Lagrangian velocity in the streamwise direction equals the Eulerian velocity located at $c\overline{Y}$, that is,

$$\frac{\mathrm{d}\overline{X}}{\mathrm{d}t} = [\overline{U}(y)]_{y=c\overline{Y}} = \frac{u^*}{\kappa} \ln \frac{c\overline{Y}}{y_0} \tag{2}$$

where y_0 is the length characterizing the wall roughness such that $\overline{U}(y)/u^* = 1/\kappa \ln(y/y_0)$. Then by combining equations (1) and (2) and integrating, Batchelor

obtained

$$\bar{X} = \frac{1}{b\kappa}\left[\bar{Y}\ln\left(\frac{c\bar{Y}}{y_0}\right) - \bar{Y} + A\right] \tag{3}$$

where A is the constant of integration which depends on the particle release position from the wall, y_T. (If the particle is released from the wall, $A = 0$). Using a crude approximation Batchelor estimated

$$A \approx y_T\left[(b-1)\ln\left(\frac{y_T}{y_0}\right) + 1 - \ln c\right]. \tag{4}$$

Equation (3) is valid only for the constant stress region and for times, $t \gg y_T/u^*$.

Batchelor also used a similarity scheme with length scale equal to $\bar{Y}$ to predict the mean concentration at ground level, C_W. By expressing the mean concentration in terms of the integral of the probability of finding a particle at a given position, he obtained the result that $C_W \propto (\Delta x u^*)^{-1}$ as $\Delta x \to \infty$.

Some of the many estimates of the constant b are as follows. Cermak [25] found good agreement of numerical calculations with various laboratory and field dispersion measurements by taking $b = 0{\cdot}1$. Values of $b \geqslant 0{\cdot}2$ gave poor agreement. Batchelor [2], using a different method, also estimated b to be less than 0·2. However, based on the argument that equation (1) must be consistent with an eddy diffusivity proportional to height, Ellison [3] and Pasquill [4] suggested $b \approx 0{\cdot}4$. Poreh and Hsu [5] discussed the possibility of b being a function of $\bar{Y}$, which contradicts the original similarity assumption.

3. FLOW FIELD

A vertical wall of a closed circuit wind tunnel (test section 10 m long and 1 × 1·2 m in cross-section) was used for the boundary-layer dispersion measurements.

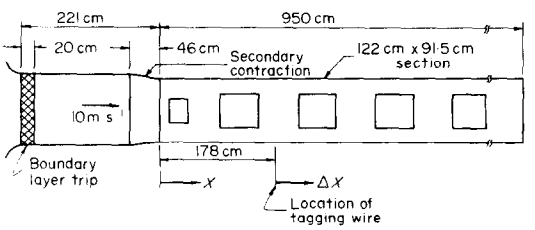

FIG. 1. Wind tunnel.

Figure 1 is a schematic sketch of the test section, including the secondary contraction of ratio 1·27 to 1 (useful for making grid-generated turbulence more nearly isotropic; Comte-Bellot and Corrsin [26]) resulting in a test section free stream velocity of 12·7 m/s. The boundary layer was tripped with commercial floor sanding paper immediately following the primary contraction. By subtracting the linearized signals of two hot wires in the flow, one wire traversing and the other stationary as a reference, the variation in free stream velocity was found to be less than 0·5 per cent at a section 1·22 m downstream of the secondary contraction exit.

The boundary-layer mean velocity profiles, measured at stations 1·78, 2·22, 2·84 and 3·46 m downstream of the secondary contraction exit fit the universal laws within the expected scatter. The RMS fluctuations compared well with Townsend's [27] at a similar Reynolds number. (Our Reynolds number based on the displacement thickness at the tagging wire was 6300.) A check for two dimensionality of the mean velocity and turbulent fluctuations at a station 3·46 m from the secondary contraction exit showed maximum variations of about 5 per cent over a transverse distance of thirty displacement thickness. However, measurements of intermittency at the 1·78 m station showed a deviation from those of others. The position of intermittency factor $= \frac{1}{2}$ occurred at $y = \delta$ while other investigators found it closer to $y = 0{\cdot}8\delta$. More details of the boundary-layer flow are described by Shlien [21].

4. APPARATUS

A platinum wire (diameter, $d_T = 0{\cdot}013$, 0·076 or 0·13 mm), stretched parallel to a vertical wall of the wind tunnel at 1·78 m downstream of the secondary contraction exit, was heated electrically with direct current, thereby tagging fluid particles. Overheat ratios of 0·3 to 0·5 were used and tension was maintained in the wire by suspending a weight from it. Using the "film" temperature (average of wire and ambient temperatures) to identify an effective kinematic viscosity, the maximum Reynolds number was computed to be less than 40 in all cases, i.e. below the critical (vortex shedding) Reynolds number.

The velocity wake behind a wire in the homogeneous turbulent shear flow ($d\bar{U}/dy = 13/s^{-1}$) of Champagne *et al.* [28] was measured (Fig. 2). This relatively long persistence of the wake is caused by the increase of production by the $-\overline{uv}(d\bar{U}/dy)$ term in the turbulent energy equation (Kellogg [29]). As a check of the effect of the finite tagging-wire diameter on the dispersion, some measurements were repeated with several wire diameters. The effect was negligible (Figs. 10, 14, and 16).

Temperature was measured using 90 per cent platinum–10 per cent rhodium resistance thermometers having a sensing element diameter 0·63 μ, and length 5 mm (resistance 3 kΩ) and 0·5 mm, operated at about 0·2 mA. The output was passed through a Honeywell model A20B, D.C. amplifier, and the mean was obtained either from a DISA 55D30 voltmeter or by integrating the signal for 90 s (set on a Cramer clock) using a calibrated chemical integrator (Self-Organizing Systems, Model SI100).

5. PROCEDURES

Velocity sensitivity of the resistance thermometer was compensated by subtracting the apparent mean temperature above ambient with the tagging wire current off from the mean temperature measured with the tagging wire current on. Typical drifts resulted in apparent temperature change of 0·003°C.

Measurements at small Δx with the source (tagging wire) on the wall ($y_T = 0$) presented special problems

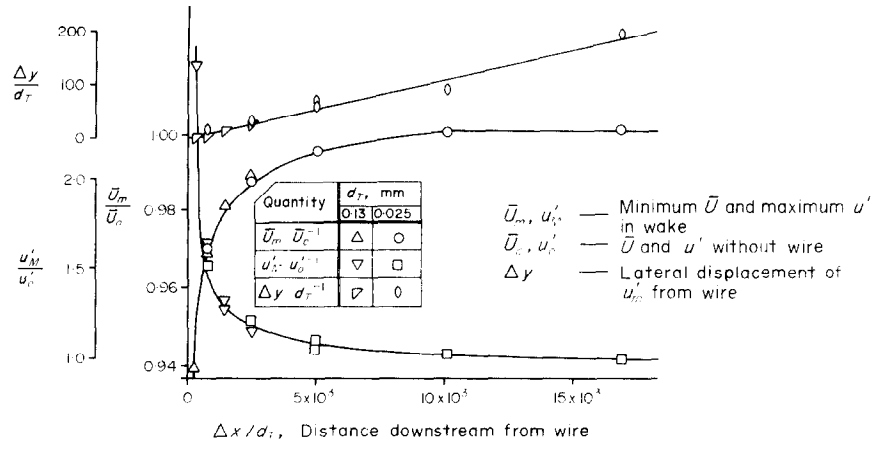

FIG. 2. Wake of wires in a homogeneous shear flow.

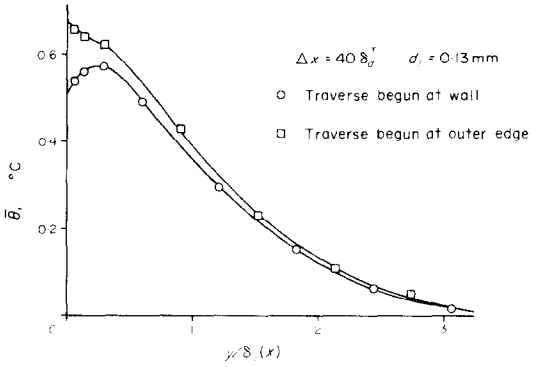

FIG. 3. Mean temperature profile with $y_T = 0$.

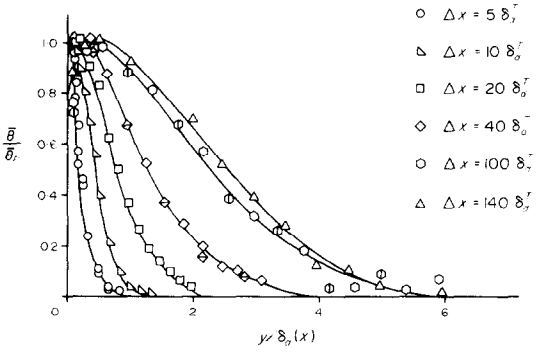

FIG. 4. Mean temperature profiles ($y_T = 0$).

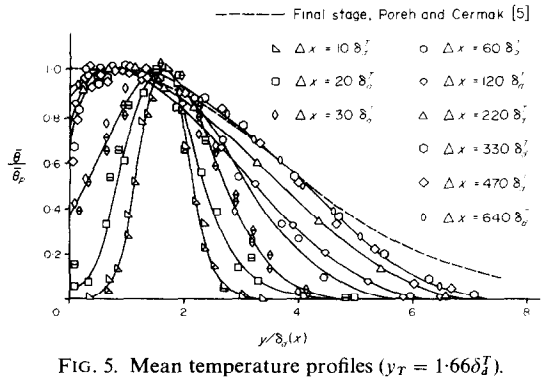

FIG. 5. Mean temperature profiles ($y_T = 1{\cdot}66\delta_d^T$).

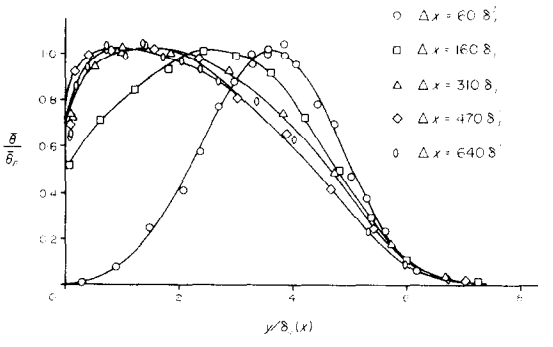

FIG. 6. Mean temperature profiles ($y_T = 4{\cdot}15\delta_d^T, \gamma \to 1$).

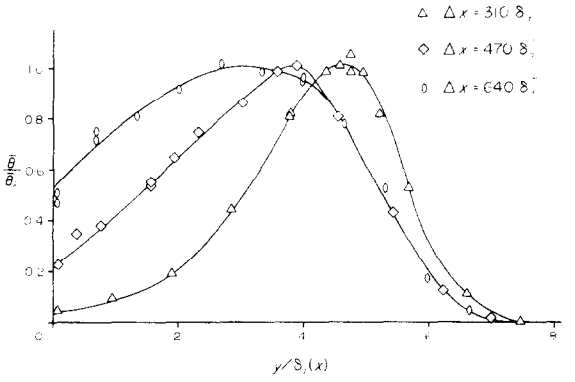

FIG. 7. Mean temperature profiles ($y_T = 7{\cdot}96\delta_d^T, \gamma = \frac{1}{3}$).

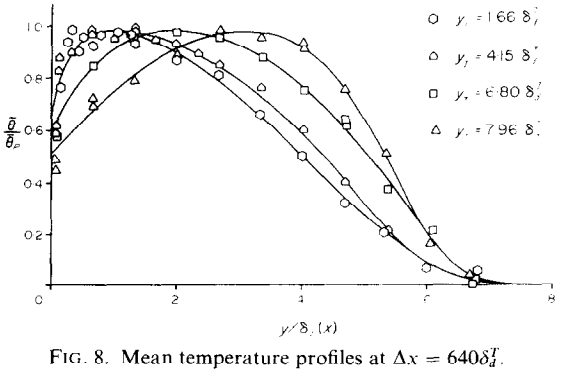

FIG. 8. Mean temperature profiles at $\Delta x = 640\delta_d^T$.

because of heat transfer from the wire (as well as the wake) to the wall (negligible in the other cases). It was found (at $\Delta x = 10\delta_d^T$, $y = 0{\cdot}33\delta_d^T$) that approximately 88 per cent of the long time asymptotic mean temperature was reached after two minutes, 92 per cent after three minutes and 98 per cent after 4 min. Far from the tagging wire, the transients were not observable. Thus, for measurements near the tagging wire, profile traverses were begun 2 min after switching the tagging wire on. Traverses were started from the wall, outwards and then back again. A typical profile is shown in Fig. 3. Since the entire traverse required about six minutes (using a DISA DVM), the upper curve is expected to be very close to the asymptotic one. Nevertheless, each of the sweeps was treated as a separate traverse in the data reduction, resulting in slight extra scatter.

6. MEAN TEMPERATURE PROFILES

Mean temperature profiles $\bar{\theta}(y)$, normalized with the peak mean temperature, $\bar{\theta}_p$ are plotted in Figs. 4–8. Distances of the source from the wall y_T, were chosen to be 0 (i.e. at the wall), $1{\cdot}66\delta_d^T(y^* \equiv u^*y/\nu = 425)$, $4{\cdot}14\delta_d^T(\gamma \to 1)$ and $7{\cdot}96\delta_d^T(\gamma = \frac{1}{2})$. Data points with the same outline but different interiors indicate different traverses of the resistance thermometer. For $y_T = 0$ the maximum Δx for which data were taken was $140\delta_d^T$, while for $y_T > 0$ the maximum Δx was $640\delta_d^T$. In comparing two curves with different y_T but with the same Δx, it should be recalled that the time of dispersion (as well as the dispersing turbulent field) is quite different in each case.

From the mean temperature profiles for $y_T > 0$, stages similar to those of Poreh and Cermak are apparent:

(i) *Initial stage*

The mean temperature profile is approximately Gaussian, like that found in unsheared homogeneous turbulence. The deviation from a Gaussian has been predicted by Hinze [30] for short times and approximately verified by Hinze and van der Hegge Zijnen [31].

(ii) *Wall stage*

The wall directly affects the temperature field $(0 < \bar{\theta} \leqslant \bar{\theta}_p)$.

(iii) *Interface stage*

This is essentially the same as Poreh and Cermak's transition stage where there is a direct effect of the turbulent-irrotational interface. This interface "lid" effect is most evident in Fig. 6 by the data collapse in the intermittent region $(y > 4{\cdot}14\delta_d)$.

(iv) *Final or asymptotic stage*

This stage is best demonstrated by the collapse of the last three $\bar{\theta}(y)$ profiles (largest Δx) in Fig. 5. Presumably the asymptotic mean temperature profile is independent of the source position.

The mean temperature profiles indicate that heat is transferred to the wall. Unfortunately this heat transfer could not be calculated to sufficient accuracy because the resistance thermometers were uncalibrated, the power dissipated by the tagging wire was not measured accurately enough, and the wall outside temperature varied by as much as 10°C. It is for these reasons that temperatures in Figs. 10–12 were normalized with the mean heat flux, Q, defined by

$$Q \equiv \int_0^\infty \frac{\bar{U}(y)}{U_\infty}\bar{\theta}(y)\,dy.$$

Scatter was reduced by this normalization.

Poreh and Cermak's final stage mean temperature profile has been plotted in Fig. 5 for comparison. The difference at the tail is considerable. Comparison in the intermediate stage is much better (Fig. 9). The data collapsed well in the range $5\delta_d^T < \Delta x < 140\delta_d^T$. The upper bound confirms Poreh and Cermak's value. For small separations, they used Weighardt's [12] data; but his smallest separation from the tagging wire was

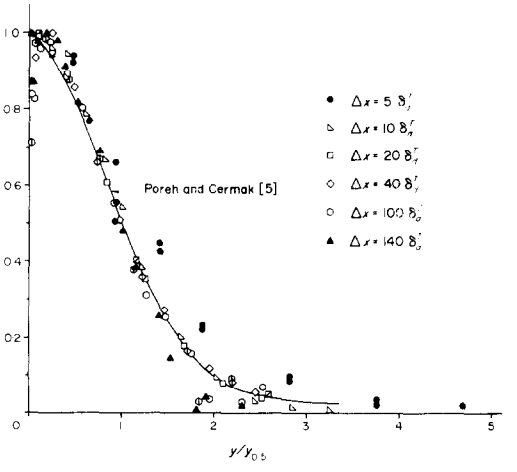

FIG. 9. Collapse of intermediate stage data ($y_T = 0$).

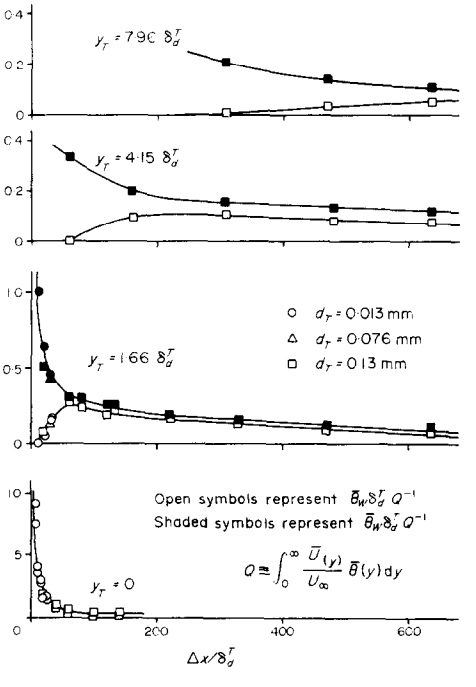

FIG. 10. Wall and peak mean temperatures.

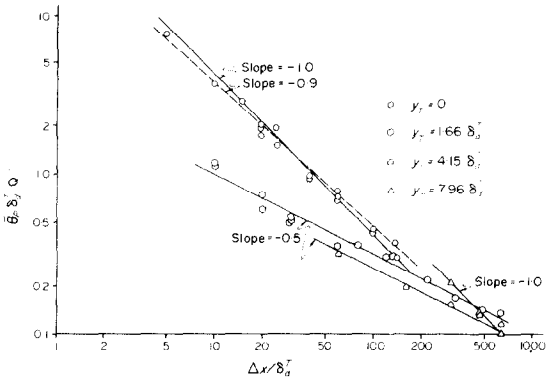

FIG. 11. Peak temperatures.

is approximately equal to $\bar{Y}$, the mean particle displacement perpendicular to the wall, and the second centroid-centered moment is approximately equal to the dispersion, $\overline{(Y-\bar{Y})^2}$. In the calculated values presented here, no correction for molecular diffusion has been attempted. Some properties of the mean temperature profiles are tabulated in Table 1 and plotted in Figs. 10–18.

(a) *Wall and peak mean temperatures*

The wall and peak mean temperatures, $\bar{\theta}_w$ and $\bar{\theta}_p$ respectively, normalized with the mean heat flux Q/δ_d^T are plotted in Fig. 10. As Δx increases $\bar{\theta}_w$ and $\bar{\theta}_p$ approach each other but $\bar{\theta}_w$ remains less than $\bar{\theta}_p$ due to heat transfer to the wall. (For $y_T = 0$, only $\bar{\theta}_w$ was plotted since it was almost equal to θ_p.) Power laws can be fitted to the $\bar{\theta}_w$ data within the scatter (Fig. 11). With the tagging wire in the interior of the boundary layer, ($y_T = 1{\cdot}66\delta_d^T$ and $4{\cdot}15\delta_d^T$), a $-1/2$ power fall-off is observed, while at the wall and in the intermittent region the power is approximately -1.

Poreh and Cermak [5] fitted a $-0{\cdot}9$ power to their data ($y_T = 0$, intermediate stage) while Batchelor [2] predicted a -1 power. It is remarkable that although Batchelor's prediction is valid for asymptotically large

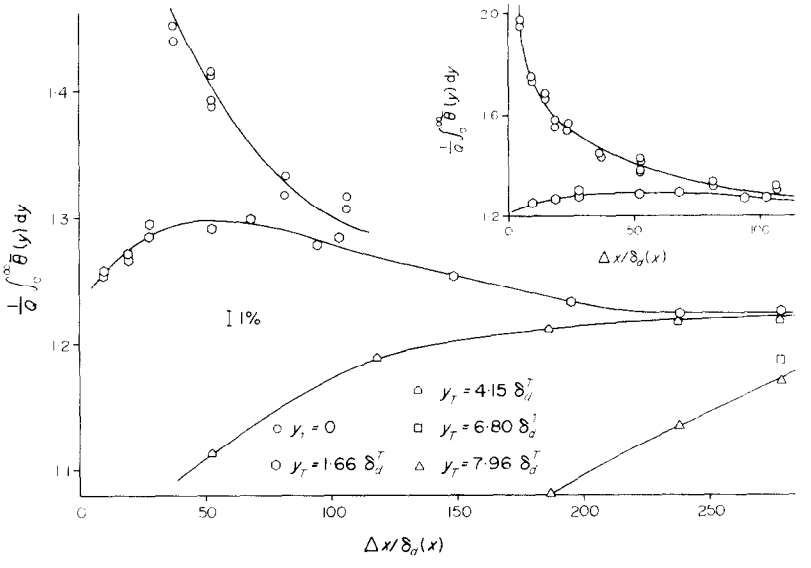

FIG. 12. Heat residing at a section.

approximately $12\delta_d^T$ and thus no lower bound was found. Hopefully our lower bound is not a result of flow disturbances caused by the tagging wire or heat transfer from the wire and wake to the wall.

7. PROPERTIES OF THE MEAN TEMPERATURE PROFILES

The mean temperature profiles can be characterized by the wall concentrations and the distance from the wall of the one-half wall concentration (both used in [5]), the peak temperature (different from the wall temperature with the tagging wire away from the wall) and the various centroid-centered moments,

$$\int_0^\infty (y-\bar{Y})^n\bar{\theta}(y)\,dy \Big/ \int_0^\infty \bar{\theta}(y)\,dy.$$

These moments are important not only as characterizations of the profiles, but also because $\bar{\theta}(y)$ is approximately equal to the probability that a particle from the source can be found at the point $(\Delta x, y)$.† Therefore, the first moment, for example, of the mean temperature profile,

$$\int_0^\infty y\bar{\theta}(y)\,dy \Big/ \int_0^\infty \bar{\theta}(y)\,dy$$

†For example, Corrsin [8] or Saffman [32].

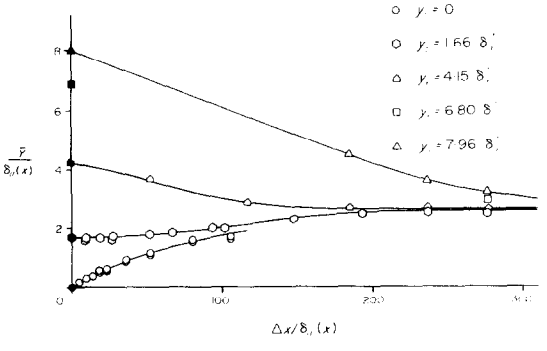

FIG. 13. Mean particles (centroid) position.

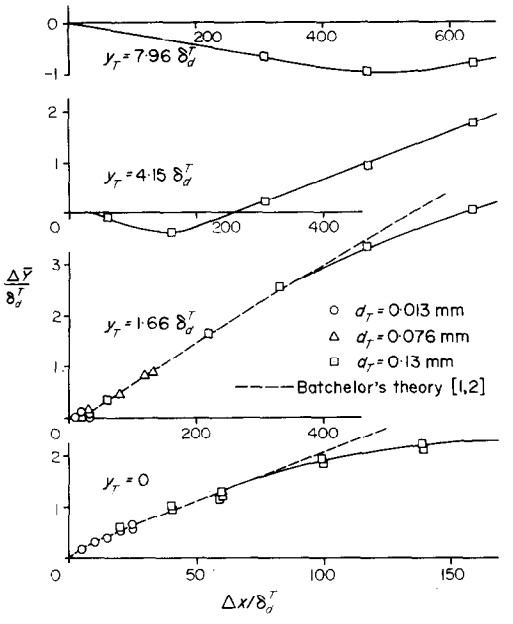

FIG. 14. Displacement of centroid.

values are 2, 4 and 50 per cent low, respectively. The latter error is partially due to the large extrapolation. The smaller deviations might be attributed to the finite tagging wire diameter. One further interesting feature is that the shapes of these curves are qualitatively the same as the wall temperature curves in Fig. 10.

(c) *Centroid position*

The centroid position has been normalized with local displacement thickness and plotted against $\Delta x/\delta_d(x)$ in Fig. 13. The curves for the various source positions appear to approach a constant, 2·54. These data are replotted in Fig. 14 as $\Delta\bar{Y}/\delta_d^T$ vs $\Delta x/\delta_d^T$, where $\Delta\bar{Y} \equiv \bar{Y} - y_T$, for comparison with Batchelor's theory. For $y_T = 4{\cdot}15\delta_d^T$ and $7{\cdot}96\delta_d^T$, the centroid initially moves towards the wall. This may be the "lid" effect of the turbulent–irrotational interface, so the theory is inappropriate here. For these cases $\Delta\bar{Y}$ begins to increase when $\bar{\theta}_w$ approaches $\bar{\theta}_p$ closest.

Batchelor's constants, A, b and c were first evaluated without regard to the restrictions of the theory. They were obtained by first calculating b from the slope of the approximately straight line portion of the curve,

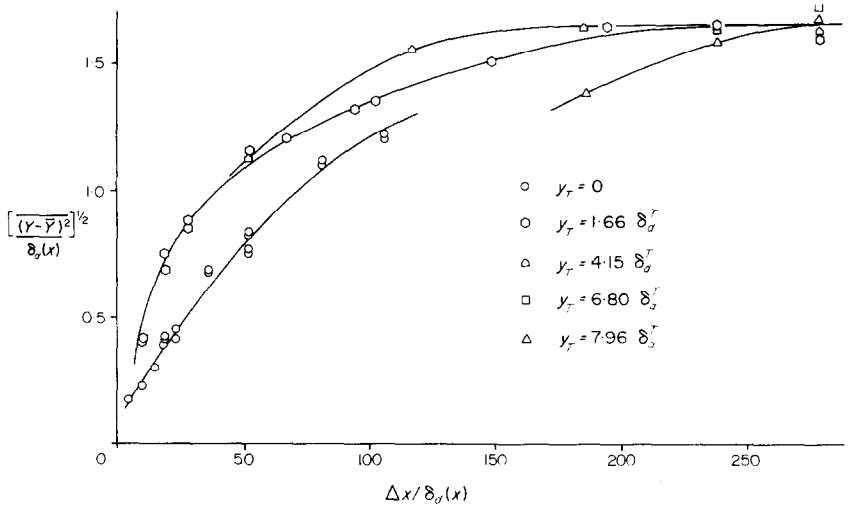

FIG. 15. Dispersion.

distances (yet within the constant stress region), the power law fits the entire range of data. Others have also measured $-0{\cdot}9$ and $-1{\cdot}0$ powers (see Pasquill [33], p. 154, and Sutton [34], p. 277).

(b) *Heat "residing" at a section*

One of the simplest characterizations of the mean temperature profile is its areas,

$$\int_0^\infty \theta(y)\,dy,$$

which is proportional to the total heat "residing" at the section. This has been normalized with the heat flux Q, for reasons mentioned, and plotted in Fig. 12. An asymptote (final stage) is approached independent of the source distance from the wall. As Δx becomes small, this normalized total heat should approach $U_\infty/\bar{U}(y_T)$, but for $y_T/\delta_d^T = 1{\cdot}66$, 4·15 and 7·96, the extrapolated and then fitting A and c by least squares.† For the tagging wire on the wall, $b = 0{\cdot}39 \pm 0{\cdot}05$, c was found to lie between 0·7 and 3·6, and A between $-0{\cdot}04$ and $-0{\cdot}08$ (apparent source position). For $y_T = 1{\cdot}66\delta_d^T$, $b = 0{\cdot}17 \pm 0{\cdot}01$, c was between 0·77 and 2·2, and A between $-3{\cdot}0$ and $-3{\cdot}5$ [equation (4) gives $A \approx -3{\cdot}3$]. The straight line portion of the $y_T = 4{\cdot}15\delta_d^T$ data resulted in $b \approx 0{\cdot}1$.

For $y_T = 0$ the b value, 0·39 agrees closely with that estimated by Ellison [3] and Pasquill [4] of 0·4, but is larger than the maximum of 0·2 estimated by Cermak [25] and Batchelor [2]. Batchelor also estimated c to be of order 1·0.

†The least square program used is "BMDX 85" of the Health Sciences Computing Facility, UCLA (revised 6 August, 1968).

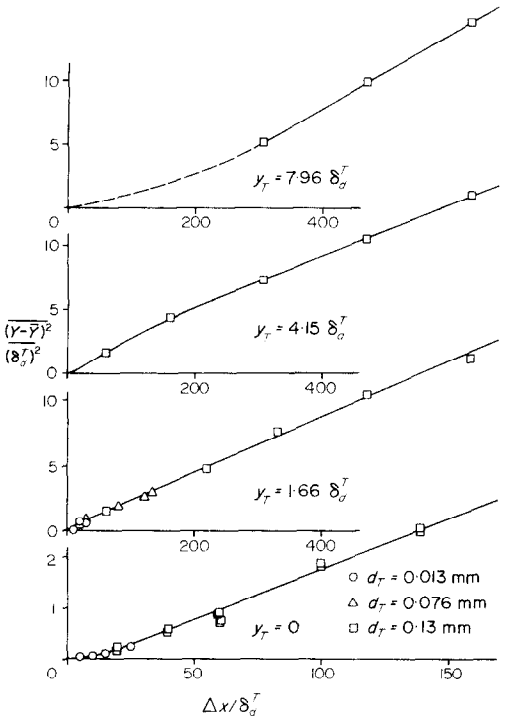

FIG. 16. Dispersion.

The theory is expected to be valid in the constant stress region and for $t \gg y_T/u^*$. If the upper limit of the constant stress region is taken as $y^* < 1000$, the first restriction results in $y < 4{\cdot}0\delta_d^T$, $3{\cdot}1\delta_d^T$ and $2{\cdot}7\delta_d^T$ for $\Delta x = 0$, $140\delta_d^T$ and $220\delta_d^T$ respectively. The $y_T = 0$ curve lies within these bounds, but for $y_T = 1{\cdot}66\delta_d^T$ the second restriction gives $t\bar{U}(y_T) \gg 33\delta_d^T$. This together with the constant stress limitation indicates that the theory is inapplicable in this case and thus there need not be any concern that the value of b here is different from that with $y_T = 0$. One other restriction implied by the constant stress assumption is that the dispersion be unaffected directly by the turbulent–irrotational interface. Thus data resulting from mean temperature profiles with tails extending well within the interface region should also be rejected, further limiting the range of validity to $\Delta x < 40\delta_d^T$ for $y_T = 0$ and $\Delta x < 30\delta_d^T$ for $1{\cdot}66\delta_d^T$.

One of the most striking aspects of the $y_T = 0$ and $1{\cdot}66\,\delta_d^T$ curves in Fig. 14 is their linearity in the constant stress region. This however, contradicts Batchelor's hypothesis that $\bar{V} = bu^* \approx$ constant [equation (1) since $\bar{V} \approx \bar{U}(\bar{Y})(\partial\bar{Y}/\partial x) \propto \bar{U}(\bar{Y})$]. The linearity of the curves also limits the usefulness of the theory since three constants are fitted to essentially a straight line.

In Fig. 18, the $\bar{Y}$ data for $y_T = 0$, extrapolated with

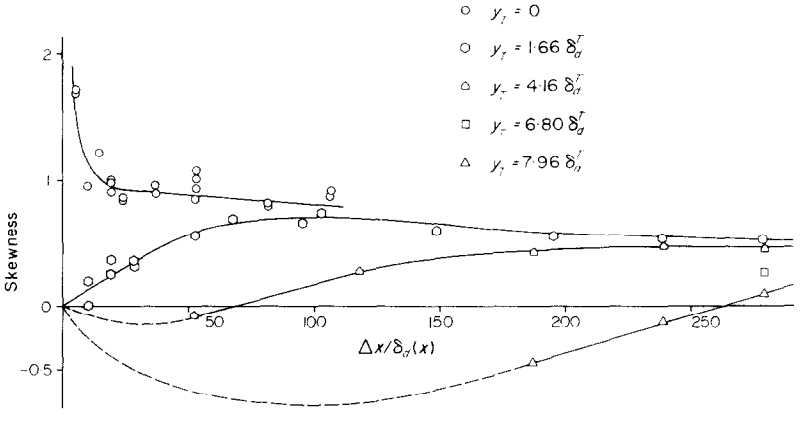

FIG. 17. Skewness of mean temperature profiles.

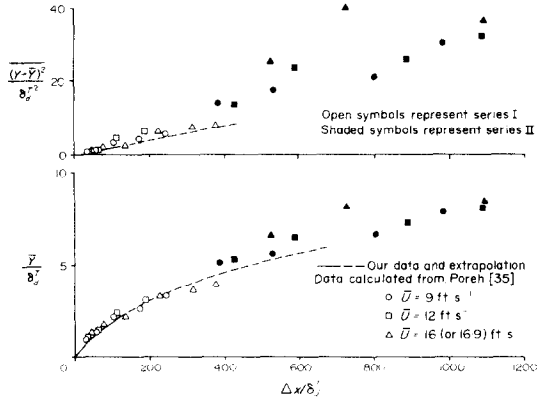

FIG. 18. Comparison with Poreh and Cermak [5].

the $y_T = 1{\cdot}66\delta_d^T$ data are compared with that of Poreh and Cermak, computed from the mean concentration profiles of Poreh [35]. The agreement is fair.

(d) *Dispersion*

The standard deviation of the mean temperature profile (square root of the particle dispersion), normalized with a local boundary-layer thickness, $[\overline{(Y-\bar{Y})^2}]^{\frac{1}{2}}/\delta_d(x)$, approaches an asymptote of approximately 1·65, as shown in Fig. 15. When $\overline{(Y-\bar{Y})^2}/(\delta_d^T)^2$ is plotted as a function of $\Delta x/\delta_d^T$ (Fig. 16) linear regions can be observed.† The small variation in the slopes as well as homogeneous turbulence analysis suggest defining a

†This contradicts the result $\overline{(Y-\bar{Y})^2} \propto \Delta t$ obtained by Chatwin [36] and others.

Table 1

$\frac{y_T}{\delta_d^T}$	$\frac{\Delta x}{\delta_d^T}$	d_T (mm)	$\frac{\bar{\theta}_p}{Q/\delta_d^T}$	$\frac{\bar{\theta}_w}{Q/\delta_d^T}$	$\frac{1}{Q}\int_0^\infty \bar{\theta}(y)\,dy$	$\frac{\Delta\bar{Y}}{\delta_d^T}$	$\frac{(Y-\bar{Y})^2}{\delta_d^{T^2}}$	Skewness
0·00	4·98	0·013	7·63	7·57	1·953	0·190	0·0298	1·69
0·00	4·98	0·013	7·63	9·15	1·974	0·188	0·0297	1·70*
0·00	9·95	0·013	3·70	3·56	1·739	0·304	0·0526	0·949
0·00	9·95	0·013	3·70	3·98	1·747	0·302	0·0527	0·952
0·00	14·9	0·013	2·87	2·75	1·671	0·391	0·0942	1·21
0·00	14·9	0·013	2·87	2·97	1·676	0·390	0·0942	1·21*
0·00	19·9	0·013	2·01	1·68	1·579	0·535	0·168	0·964
0·00	19·9	0·13	1·78	1·72	1·558	0·567	0·185	0·905
0·00	19·9	0·13	1·99	1·96	1·577	0·540	0·180	0·984
0·00	24·9	0·013	1·53	1·58	1·544	0·637	0·225	0·854
0·00	24·9	0·013	1·96	1·79	1·567	0·587	0·192	0·839
0·00	39·8	0·13	0·944	0·843	1·439	0·994	0·561	0·904
0·00	39·8	0·13	0·997	0·962	1·450	0·963	0·543	0·948
0·00	59·7	0·13	0·725	0·352	1·392	1·22	0·759	0·854
0·00	59·7	0·13	0·794	0·688	1·422	1·16	0·748	0·933
0·00	59·7	0·13	0·709	0·376	1·389	1·27	0·885	1·01
0·00	59·7	0·13	0·785	0·642	1·414	1·21	0·868	1·07
0·00	99·5	0·13	0·441	0·304	1·318	1·92	1·87	0·785
0·00	99·5	0·13	0·454	0·425	1·334	1·85	1·82	0·813
0·00	139·0	0·13	0·368	0·303	1·308	2·20	2·53	0·876
0·00	139·0	0·13	0·373	0·373	1·317	2·14	2·48	0·917
1·66	9·95	0·013	1·19	0·0000	1·254	0·000	0·173	0·000
1·66	9·95	0·013	1·21	0·0000	1·256	−0·015	0·177	0·192
1·66	19·9	0·013	0·761	0·0590	1·267	0·047	0·511	0·380
1·66	19·9	0·13	0·616	0·0897	1·272	0·046	0·609	0·249
1·66	29·9	0·013	0·530	0·192	1·295	0·008	0·830	0·360
1·66	29·9	0·013	0·539	0·158	1·284	0·061	0·815	0·333
1·66	29·9	0·076	0·514	0·153	1·278	0·126	0·877	0·325
1·66	59·7	0·13	0·358	0·331	1·291	0·343	1·71	0·561
1·66	79·6	0·076	0·366	0·292	1·298	0·450	2·02	0·685
1·66	119·0	0·076	0·305	0·230	1·278	0·818	2·79	0·645
1·66	133·0	0·076	0·302	0·261	1·283	0·866	3·05	0·729
1·66	219·0	0·13	0·222	0·198	1·253	1·64	4·94	0·583
1·66	332·0	0·13	0·168	0·153	1·233	2·54	7·85	0·554
1·66	471·0	0·13	0·142	0·0923	1·222	3·36	10·7	0·536
1·66	637·0	0·13	0·124	0·0682	1·225	4·06	13·6	0·515
4·15	59·7	0·13	0·330	0·0003	1·114	−0·114	1·64	−0·081
4·15	159·0	0·13	0·198	0·0951	1·190	−0·380	4·40	0·270
4·15	308·0	0·13	0·155	0·105	1·211	0·213	7·34	0·411
4·15	471·0	0·13	0·133	0·0790	1·219	0·936	10·6	0·470
4·15	637·0	0·13	0·117	0·0728	1·219	1·77	14·1	0·448
6·80	637·0	0·13	0·101	0·0595	1·187	−0·028	15·5	0·265
7·96	308·0	0·13	0·209	0·0078	1·081	−0·663	5·23	−0·455
7·96	471·0	0·13	0·139	0·0308	1·135	−0·950	9·88	−0·138
7·96	637·0	0·13	0·102	0·0500	1·170	−0·775	14·7	0·096

*Same data as previous case but different extrapolation to the wall.

turbulent diffusivity by $U_\infty(\partial/\partial x)\frac{1}{2}\overline{(Y-\bar{Y})^2}$.† A turbulent Prandtl number (ratio of momentum to thermal turbulent diffusivities) can thus be defined using a typical turbulent viscosity for the boundary layer of $0{\cdot}6u^*\delta$ (see, for example, Hinze [37] Figs. 7–17). The resulting Prandtl numbers 0·80, 0·73, 0·82, 0·56 for $y_T/\delta_d^T = 0$, 1·66, 4·15 and 7·96 respectively are not far from the "Reynolds analogy" (see, for example, Monin and Yaglom [20], p. 341) value of 1. Unity is approximately the generally "accepted" turbulent Prandtl number (based on the *usual* definition of turbulent diffusivity). (See, for example, [20], pp. 332 and 337.)

The data are also compared with those of Poreh and Cermak in Fig. 18. The slope of their $\overline{(Y-\bar{Y})^2}$ data is approximately the same as ours but their values, like those for $\bar{Y}$, are larger. The data for their series II experiments (source located 7·8 m from the boundary layer trip) differ, beyond the scatter, from their series I experiments (source 2·8 m from the trip), showing some effect of source location.

The skewness, $\overline{(Y-\bar{Y})^3}/[\overline{(Y-\bar{Y})^2}]^{3/2}$, in Fig. 17, demonstrates the approach to an asymptote.

†This diffusivity is different from the usual one defined by $-\overline{v\theta}/(\partial\bar{\theta}/\partial y)$.

CONCLUSIONS

1. The normalized mean temperature profiles approached an asymptotic form, independent of the source (tagging wire) distance from the wall.

2. Power laws fitted to the mean wall concentrations (temperatures) as functions of downstream distance,

resulted in an approximately -1 power for the source on the wall or in the intermittent region, and a $-1/2$ power for the source completely within the turbulent region. The wall source result is essentially the same as Poreh and Cermak's [5].

3. The centroid position, $\overline{Y}$, as a function of Δx agreed approximately with that calculated from Poreh's [35] data. The measured value of the constant b in Batchelor's [1], [2] analysis agreed closely with the estimates of Ellison [3] and Pasquill [4] for $y_T = 0$. The restrictions of the theory were not satisfied for the other source positions. The hypothesis that $\mathrm{d}\overline{Y}/\mathrm{d}t \propto u^*$ was contradicted by the data.

4. Probably the most useful and interesting result of these measurements was the variation of the centroid-centered second moment, $\overline{(Y-\overline{Y})^2}$, with Δx and y_T. By defining a turbulent diffusivity as $U_\infty(\partial/\partial x)\frac{1}{2}\overline{(Y-\overline{Y})^2}$, and using an average (across the boundary layer) turbulent viscosity, a Prandtl number was defined. This turbulent Prandtl number was not far from the "Reynolds analogy" value of 1 (0·6 to 0·8) and showed little variation with y_T.

5. Because $\overline{Y}$ and $\overline{(Y-\overline{Y})^2}$ change with respect to Δx at different rates, it seems unlikely that the data could be collapsed onto a single curve using a simple rescaling scheme.

Acknowledgement—This work was supported primarily by the Atomic Energy Commission contract AEC AT(111)3284. Some data reduction and initial manuscript preparation was done while DJS was in the Department of Chemical Engineering at the University of British Columbia supported by NRC grant number A4936. The manuscript was completed at the University of Tel-Aviv with support from AFOSR (NAM) Project No. 9781-01.

REFERENCES

1. G. K. Batchelor, Some reflections on the theoretical problems raised at the symposium, *Adv. Geophys.* **6**, 449 (1959).
2. G. K. Batchelor, Diffusion from sources in a turbulent boundary layer, *Arch. Mech. Stos.* **3**(16), 661 (1964).
3. T. H. Ellison, Turbulent diffusion, *Sci. Prog., Lond.* **47**,
2. G. K. Batchelor, Diffusion from sources on a turbulent boundary layer, *Arch. Mech. Stos.* **3**(16), 661 (1964).
3. T. H. Ellison, Turbulent diffusion, *Sci, Prog. Lon.* **47**, 495 (1959).
4. F. Pasquill, Lagrangian similarity and vertical diffusion from a line source at ground level, *Q. Jl R. Met. Soc.* **92**, 185 (1966).
5. M. Poreh and J. E. Cermak, Study of diffusion from a line source in a turbulent boundary layer, *Int. J. Heat Mass Transfer* **7**, 1083 (1964).
6. G. K. Batchelor, Note on free turbulent flows, with special reference to the two-dimensional wake, *J. Aeronaut. Sci.* 441–445 (1950).
7. S. Corrsin, Some current problems in turbulent shear flow, in *Symposium on Naval Hydrodynamics* (edited by F. S. Sherman) 373, Publ. 515. Nat. Acad. Sci./Nat. Res. Council, Washington, D.C. (1957).
8. S. Corrsin, Theories of turbulent dispersion, Proc. Intern. Colloq. on Turbulence, Centr. Nat. Rech. Sci., 27, Marseille (1961).
9. M. V. Morkovin, On eddy diffusivity, quasi-similarity and diffusion experiments in turbulent boundary layers, *Int. J. Heat Mass Transfer* **8**, 129 (1965).
10. H. K. Skramstad and G. B. Schubauer, The application of thermal diffusion to the study of turbulent air flow, *Phys. Rev.* **53**(11), 927 (1938).
11. H. L. Dryden, Turbulence and diffusion, *Ind. Engng Chem.* **33**(4), 416 (1939).
12. K. Wieghardt, Uber Ausbreitungsvorgange in turbulenten Reibungsschichten, *Z. Angew. Math. Mech.* **28**(1), 346 (1948).
13. D. M. Kesic, Diffusion of heat from an instantaneous point source in a turbulent boundary layer, Tech. Rep. CER66-67DK45, College of Engineering, Colorado State University (1966).
14. S. Chandra, Some features of instantaneous point source diffusion within a turbulent boundary layer, *Tellus* **24**, 230 (1972).
15. F. H. Chaudhry and R. N. Meroney, Turbulent diffusion in a stably stratified shear layer, Tech. Rep. C-0423-5, College of Engineering, Colorado State University (1969).
16. D. S. Johnson, Velocity, temperature and heat-transfer measurements in a turbulent boundary layer downstream of a stepwide discontinuity in wall temperature, *J. Appl. Mech.* **24E**, 2 (1957).
17. D. S. Johnson, Velocity and temperature fluctuation measurements in a turbulent boundary layer downstream of a stepwise discontinuity in wall temperature, *J. Appl. Mech.* **26E**, 325 (1959).
18. C. I. H. Nicholl, Some dynamical effects of heat on a turbulent boundary layer, *J. Fluid Mech.* **40**, 361 (1970).
19. M. Trinite and P. Valentin, Couche limite turbulente avec discontinuite de temperature et de concentration a la paroi, *Int. J. Heat Mass Transfer* **15**, 1337–1354 (1972).
20. A. S. Monin and A. M. Yaglom, *Statistical Fluid Mechanics: Mechanics of Turbulence* Vol. 1. MIT Press, Cambridge (1971).
21. D. J. Shlien, Dispersion measurements of a fluid sheet in two turbulent flows, Ph.D. dissertation, The Johns Hopkins University (1971).
22. S. Corrsin and A. L. Kistler, Free stream boundaries of turbulent flows, NACA Rep. 1244 (1955).
23. M. Poreh and K. S. Hsu, Diffusion from a line source in a turbulent boundary layer, *Int. J. Heat Mass Transfer* **14**, 1473 (1971).
24. F. A. Gifford, Diffusion in the diabatic surface layer, *J. Geophys. Res.* **67**(8), 3027 (1962).
25. J. E. Cermak, Lagrangian similarity hypothesis applied to diffusion in turbulent shear flow, *J. Fluid Mech.* **15**, 49 (1963).
26. G. Comte-Bellot and S. Corrsin, The use of a contraction to improve isotropy of grid-generated turbulence, *J. Fluid Mech.* **25**, 657 (1966).
27. A. A. Townsend, The structure of the turbulent boundary layer, *Proc. Camb. Phil. Soc.* **47**, 375 (1951).
28. F. H. Champagne, V. G. Harris and S. Corrsin, Experiments on nearly homogeneous turbulent shear flow, *J. Fluid Mech.* **41**, 81 (1970).
29. R. M. Kellogg, Evolution of a spectrally local disturbance in a grid-generated turbulent flow, Ph.D. Thesis, The Johns Hopkins University (1965).
30. J. O. Hinze, Turbulent diffusion from a source in turbulent shear flow, *J. Aeronaut. Sci.* **18**(8), 565 (1951).
31. J. O. Hinze and van der Hegge Zijnen, Local transfer of heat in anisotropic turbulence, in *General Discussion on Heat Transfer*, Inst. of Mech. Engng, ASME, New York (1951).
32. P. G. Saffman, An approximate calculation of the Lagrangian auto-correlation coefficient for stationary homogeneous turbulence, *Appl. Scient. Res.* **11A**, 245 (1963).
33. F. Pasquill, *Atmospheric Diffusion*. D. van Nostrand, New York (1962).
34. O. G. Sutton, *Micrometeorology*. McGraw-Hill, New York (1953).
35. M. Poreh, Diffusion from a line source in a turbulent

boundary layer, Ph.D. dissertation, Colorado State University (1961).
36. P. C. Chatwin, The dispersion of a puff of passive contaminant in the constant stress region, *Q. Jl R. Met. Soc.* **94**(401), 350 (1968).
37. J. O. Hinze, *Turbulence*. McGraw-Hill, New York (1959).

MESURES DE DIFFUSION DANS LA COUCHE LIMITE TURBULENTE

Résumé—On a mesuré la diffusion dans la couche limite turbulente en soufflerie, en aval d'un long fil chauffé, placé successivement à la paroi, à une distance de la paroi égale à 1,66 fois l'épaisseur de déplacement, à une position au-delà de laquelle l'intermittence tombe au dessous de 1,0 et enfin dans la région intermittente. Dans tous les cas les profils de température approchaient à peu près la même forme asymptotique. Le nombre de Prandtl turbulent défini par

$$\left\{\frac{U_\infty}{\nu_t}\frac{\partial}{\partial x}\tfrac{1}{2}\overline{(Y-\bar{Y})^2}\right\}^{-1}$$

n'est pas éloigné (0,6 à 0,8) de la valeur 1 donnée par l'analogie de Reynolds. De plus, ce nombre de Prandtl turbulent est approximativement indépendant de la position en aval et varie peu avec la distance de la source à la paroi. Les concentrations (ou températures) moyennes pariétales ont été approchées par de simples lois puissance en fonction de la distance aval. La constante b relative au déplacement moyen de la particule perpendiculairement à la paroi, dans la théorie de Batchelor [1, 2], a été calculée à partir des données sur la source placée en paroi, quoiqu'une hypothèse fondamentale de la théorie ($\bar{V} \approx$ constante) soit en contradiction avec les données. La valeur de b est en bon accord avec l'estimation de Ellison [3] et Pasquill [4]. Les restrictions de la théorie n'étaient pas satisfaites pour les autres positions de la source. La comparaison avec les mesures de Poreh et Cermak [5] (approximativement au même nombre de Reynolds) a montré l'existence de certains domaines d'accord.

DISPERSIONSMESSUNGEN IN EINER TURBULENTEN GRENZSCHICHT

Zusammenfassung—Die Dispersion in einer turbulenten Grenzschicht wurde in einem Windkanal gemessen stromabwärts eines langen beheizten Drahtes an der Wand in einer Entfernung von der Wand vom 1,66-fachen der Verdrängungsdicke, sowohl im Schwankungsbereich als auch jenseits des Bereiches in dem die Schwankungen unter den Wert 1,0 abfallen. Die mittleren Temperaturprofile nahmen in allen Fällen etwa die gleiche asymtotische Form an. Eine turbulente Prandtl-Zahl, definiert nach

$$\left[\frac{U_\infty}{\nu_t}\frac{\partial}{\partial x}\tfrac{1}{2}\overline{(Y-\bar{Y})^2}\right]^{-1}$$

lag nicht weit vom "Reynolds-Analogie"-Wert von 1 (0,6–0,8) entfernt. Diese turbulente Prandtl–Zahl war angenähert unabhängig von der Lage stromabwärts und ergab wenig Änderung bei geändertem Quellabstand von der Wand. Die mittleren Wandkonzentrationen (Temperaturen als Funktion des Abstandes stromabwärts) wurden mit einfachen Exponentialgesetzen angespasst. Die Konstante b in Batchelor's Theorie [1, 2] für die mittlere Teilchenverdrängung senkrecht zur Wand, wurde berechnet aus den Daten der Quelle an der Wand, obwohl die grundsätzliche Annahme der Theorie ($\bar{V} \approx$ konstant) von den Ergebnissen widerlegt wurde. Der Wert b stimmte sehr gut überein mit den Schätzungen von Ellison [3] und Pasquill [4]. Einschränkungen der Theorie wurden durch andere Quellanordnungen nicht befriedigt. Der Vergleich mit Messungen von Poreh und Cermak [5] (bei etwa gleichen Reynolds–Zahlen) ergab einige Bereiche der Übereinstimmung.

ИЗМЕРЕНИЕ ДИСПЕРСИИ В ТУРБУЛЕНТНОМ ПОГРАНИЧНОМ СЛОЕ

Аннотация — Измерения дисперсии в турбулентном пограничном слое проводились в аэродинамической трубе за длинной нагретой проволокой, которую располагали последовательно на стенке, на расстоянии 1,66 толщины вытеснения от стенки, в месте, за пределами которого величина перемежаемости падала ниже 1,0, а также в области перемежаемости. Во всех случаях средние профили скорости приближались к почти одному и тому же асимптотическому виду. Значение турбулентного числа Прандтля, определяемого выражением

$$\left[\frac{U_\infty}{\nu_t}\frac{\partial}{\partial x}\frac{1}{2}\overline{(y-\bar{y})^2}\right]^{-1},$$

не отличалось намного от значения, которое следует из «аналогии Рейнольдса», равного 1 (от 0,6 до 0,8). Кроме того, значение турбулентного числа Прандтля почти не зависело от положения проволоки вдоль по потоку и незначительно изменялось с расстоянием от стенки. Зависимость средних значений концентрации на стенке (температур) от расстояния вниз по потоку описывается простыми степенными закономерностями. Константа «b» в теории Бэтчелора [1,2] для среднего вытеснения частицы перпендикулярно к стенке рассчитывалась по данным, полученным для источника на стенке, хотя результаты не подтвердили основную гипотезу теории Бэтчелора ($\bar{V} \approx$ constant). Значение константы «b» хорошо согласуется с оценками Эллисона [3] и Паскилля [4]. Ограничения теории не получили подтверждения в случае других местоположений источника. Получено некоторое согласие с результатами измерений Порека и Чермака [5] примерно при том же значении числа Рейнольдса.